

## Supplementary Figure Legends

### **Fig S1. Extended comparison of the accuracy of different deconvolution methods (see Fig 1b for description).**

**a** Heatmaps indicate the spatial distribution of different cell types. The true frequency (blue) are compared with estimates from different deconvolution methods (red). The RMSE corresponding to each cell type is indicated.

**b** Scatter plot indicate the relationship between true (y-axis) and inferred (x-axis) cell type frequencies. Results from all the cell types are overlaid. The overall level of RMSE is indicated for each method.

### **Fig S2. Deconvolution analysis of the mouse brain Visium dataset.**

**a** The spatialDWLS estimated spatial distribution of different cell types (indicated as red dots).

**b.** The anatomic structure of the brain, obtained from the Allen Brain Atlas, is shown here for comparison with the deconvolution analysis results.

### **Fig S3. Deconvolution analysis of the human developing heart Spatial Transcriptomic dataset.**

SpatialDWLS estimated spatial distribution of atrial cardiomyocytes, ventricular cardiomyocytes, smooth muscle cells and epicardium derived cells in week 4.5-5 (**a**), week 6.5 (**b**) and week 9 (**c**). The magnitude of cell-type frequency at each spot is indicated by red circles.

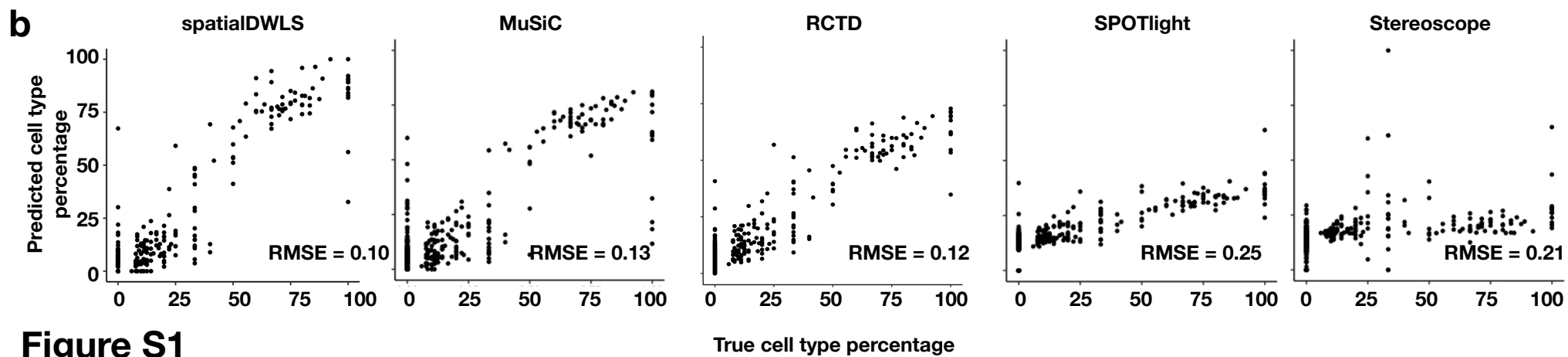
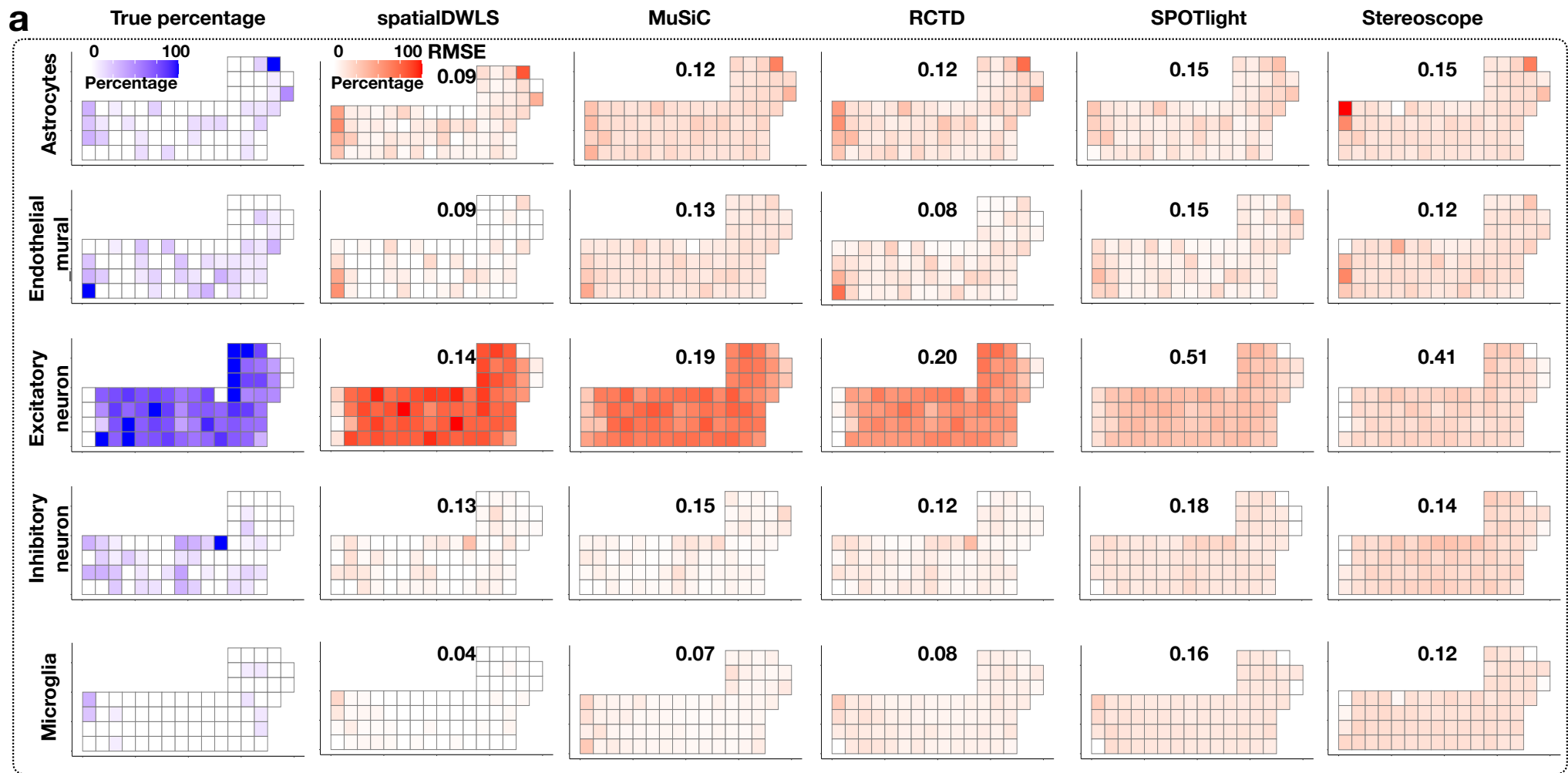


**Figure S1**

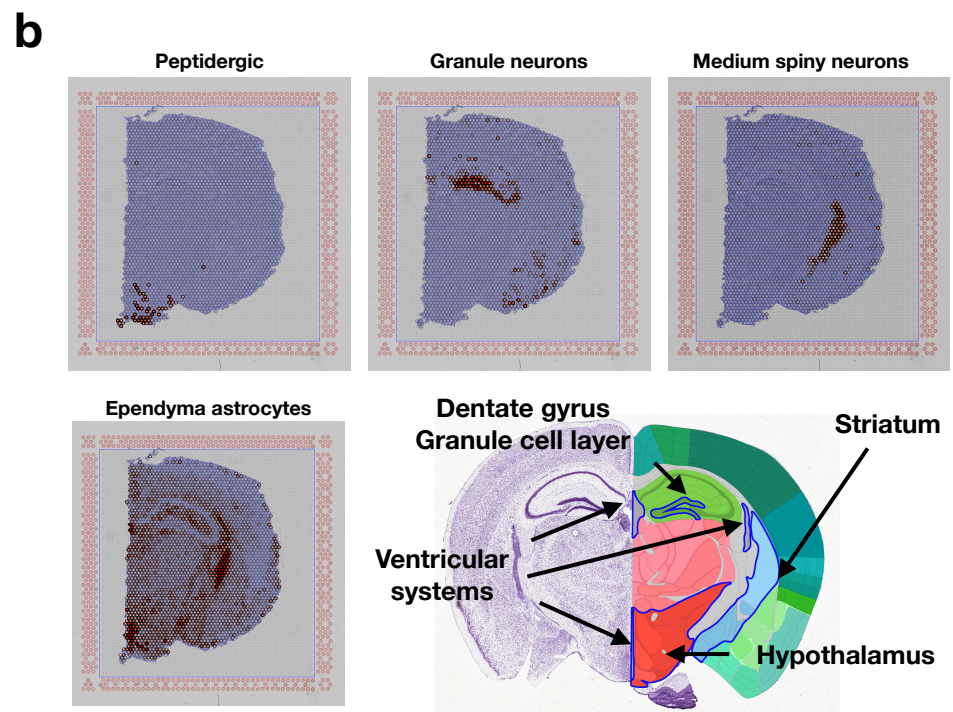
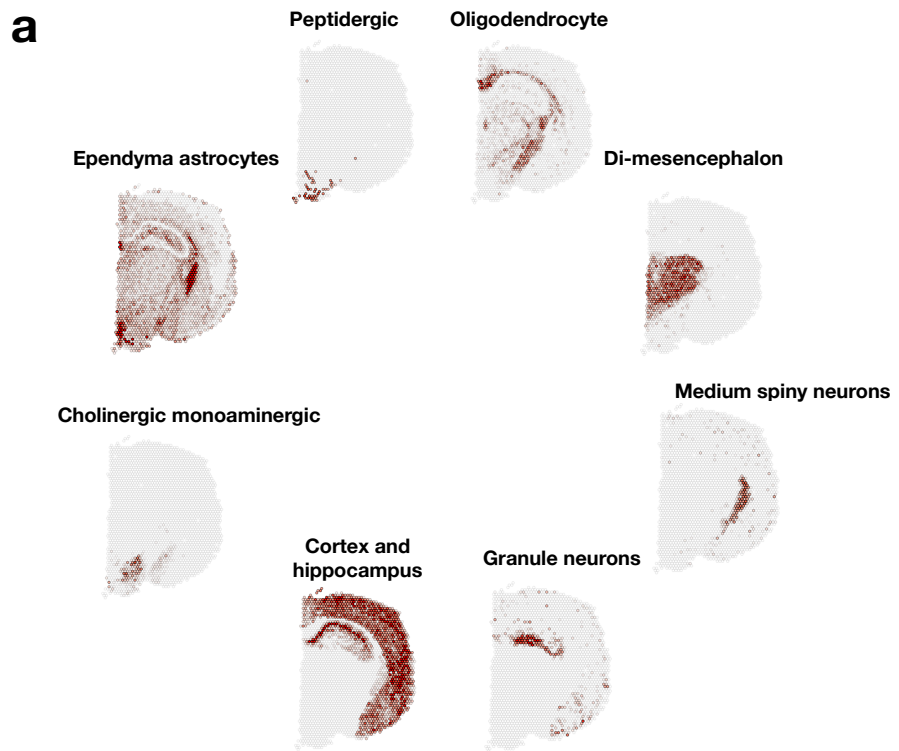


**Figure S2**

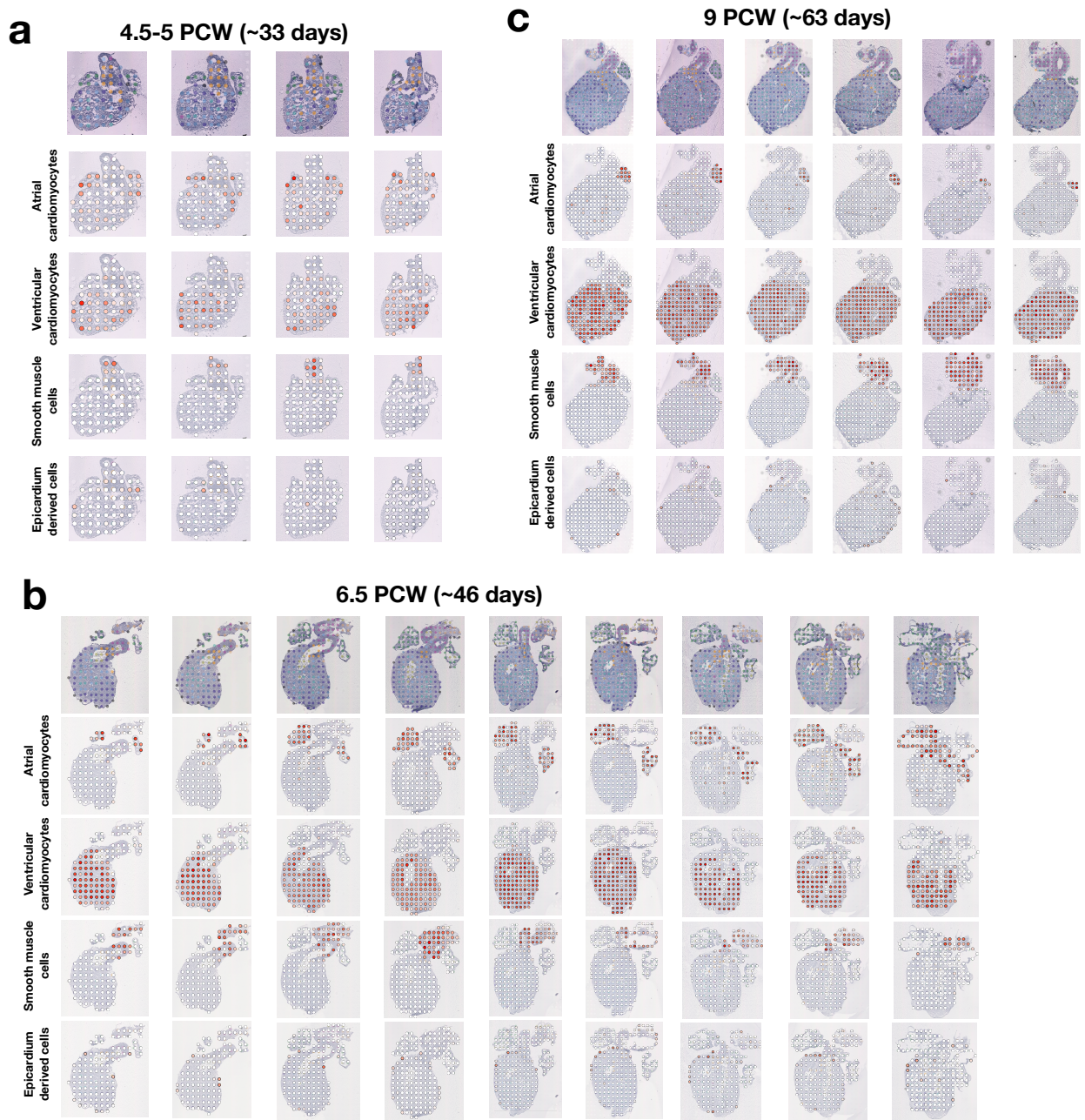


**Figure S3**